

# Comparison of SANC with KORALZ and PHOTOS \*

A. Andonov<sup>a</sup>, S. Jadach<sup>b</sup>, G. Nanava<sup>a</sup> and Z. Was<sup>b,c</sup>

<sup>a</sup> Lab. of Nuclear Problems, JINR, RU-141980 Dubna, Russia

<sup>b</sup> Institute of Nuclear Physics, ul. Radzikowskiego 152, PL-31-342 Cracow, Poland

<sup>c</sup> CERN, Theory Division, CH-1211 Geneva 23, Switzerland

January 15, 2003

## Abstract

Using the SANC system we study the one-loop electroweak standard model prediction, including virtual and real photon emissions, for the decays of on-shell vector and scalar bosons  $B \rightarrow f\bar{f}(\gamma)$ , where  $B$  is a vector boson,  $Z$  or  $W$ , or a Standard Model Higgs. The complete one-loop corrections and exact photon emission matrix element are taken into account. For the phase-space integration, the Monte Carlo technique is used. For  $Z$  decay the QED part of the calculation is first cross-checked with the exact one-loop QED prediction of KORALZ. For Higgs boson and  $W$  decays, a comparison is made with the approximate QED calculation of PHOTOS Monte Carlo. This provides a useful element for the evaluation of the theoretical uncertainty of PHOTOS, very interesting for its application in ongoing LEP2 and future LC and LHC phenomenology.

## 1. Introduction

The SANC project of Ref. [1] has several purposes. The intermediate goal is to summarize and consolidate the effort of the last three decades in calculating Standard Model radiative corrections for LEP, in a well organized calculational environment for future reference. However, it is aimed not only at training young researchers and students, but at some remaining calculational projects for LEP as well.

SANC provides an Internet-oriented, graphic interface platform, which is meant to serve as a starting point for longer term research efforts in the area of the higher order (multi-loop) calculations within the SM and beyond, for the experiments at future high energy colliders. An important lesson from the LEP experiments [2] is that the desirable way of providing theoretical predictions is in the form of Monte Carlo event generators. This

---

\*Work supported in part by the European Union 5-th Framework under contract HPRN-CT-2000-00149, Polish State Committee for Scientific Research (KBN) grant 2 P03B 001 22, NATO grant PST.CLG.977751 and INTAS M<sup>o</sup> 00-00313.

aspect has been taken into account in the development of **SANC** from an early stage of its development.

The currently available version of **SANC** can construct one-loop spin amplitudes for the decays of the gauge bosons  $W$  and  $Z$  and Higgs boson  $H$ . All of the Born and one-loop-corrected spin amplitudes are generated interactively from scratch<sup>1</sup> by **SANC** with the help of the algebraic package **Form3** [4] in the form of Fortran77 source codes, and are then used in the MC generation/integration part of the package. For the moment, **SANC** features single real photon emission, in the calculations of the total rate and decay spectra of the  $B \rightarrow f\bar{f}(\gamma)$  process. The complete spin polarization density matrix of the decaying boson is taken into account as well.

The integration, with the Monte Carlo method, over the three (two)-body final state is done without any approximation (in particular small mass approximation is not used). The program provides MC events with constant weight (unweighted events). The whole system is, therefore, fairly self-contained and complete<sup>2</sup>.

It is of the utmost importance for such a new system to precisely reproduce known results. Concerning virtual corrections, comparisons were performed with the calculations of refs. [5,6]. The precise comparisons with the **FeynArt** package [7] were made in [8–10] as well.

Our paper is organized as follows: in the next section we describe in detail the set of observables chosen for tests and the input parameter set-ups for comparisons **SANC** with **KORALZ** [11] and **SANC PHOTOS** [12]. Section 3 is devoted to a discussion of **SANC** technical reliability in the domain of QED bremsstrahlung. To this end, comparisons with **KORALZ** and leading-log distributions from **PHOTOS** are collected. Section 4 describes comparisons of **SANC** with **PHOTOS**, focusing on the non-leading contributions in  $W$  and  $H$  decays and on the relevant discussion of **PHOTOS** physical uncertainties. The summary in section 5 closes the paper.

## 2. Initialization set-ups for **SANC**, **KORALZ** and **PHOTOS** runs

In the following sections we compare predictions from the programs **SANC**, **KORALZ** and **PHOTOS**. It is essential that the initialization be identical in all cases and close to the physical reality; in particular the following options are set in the three programs:

- In **SANC** we switch off the EW part of the radiative corrections. The soft photon limit is kept at 0.005 of the decaying particle mass.
- In **KORALZ** we switch to the  $\mathcal{O}(\alpha)$  mode of operation (no exponentiation) with final state bremsstrahlung only. We set the CMS energy equal to the  $Z$  mass. The  $s$ -

---

<sup>1</sup>The **form2** codes related to the review of ref. [3] were exploited at the early stage of the **SANC** development.

<sup>2</sup>That is why it may be valuable for teaching and training.

channel  $\gamma$  exchange is switched off and the soft photon limit is kept at 0.01 of the “beam energy”.

- In PHOTOS we switch off the double bremsstrahlung corrections but we keep interference effects. The soft/hard photon limit is kept at 0.005 of the decaying particle mass. For the generation of the Born-level two-body decays, we use the Monte Carlo generation from SANC.

To visualize the differences (or the agreement) between the calculations, we choose a certain class of (pseudo-)observables, more precisely the one-dimensional distributions, which are quite similar to the one used in the first tests of PHOTOS reported in [13]. To visualize the usually small differences, we plot ratios of the predictions from two programs rather than the distributions themselves.

List of observables:

- **-A-** *Photon energy in the decaying particle rest frame:* this observable is sensitive mainly to the leading-log (i.e. collinear) non-infrared (i.e. not soft) component of the distributions.
- **-B-** *Energy of the final state charged particle:* as in the previous case this observable is sensitive mainly to the leading-log (i.e. collinear) non-infrared (i.e. not soft) component of the distributions.
- **-C-** *Angle of the photon with respect to one of the charged final state particles:* this observable is sensitive mainly to the non-collinear (i.e. non-leading-log) but soft (i.e. infrared) component of the distributions.
- **-D-** *Acollinearity angle of the final state charged particles:* this observable is sensitive mainly to the non-collinear (i.e. non-leading-log) and non-soft (i.e. non-infrared) component of the distributions.

### 3. Technical tests of SANC

Let us first cross check SANC predictions in the case of  $Z \rightarrow \mu^+ \mu^-$  decay and for the real photon emission with KORALZ. The corresponding part of the KORALZ code, essentially an improved emulation of the MC program MUSTRAL [14], was thoroughly tested over two decades and is an excellent candidate for the benchmark test for SANC matrix-element and phase-space generation. It can be noted that the phase-space parametrization of the single photon emission in SANC, although developed independently, is essentially the same as in KORALB [15–17].

As we can see from figs. 1 and 2 the level of the agreement for all distributions of the types **A**, **B**, **C** and **D** is satisfactory, at the level of better than 0.5% (or at the level of statistical error). We have checked that the  $\mathcal{O}(\alpha)$  FSR correction to the total decay rate calculated as a difference of SANC results, with FSR on and off, agrees well with the

standard factor  $1 + \frac{3}{4}\frac{\alpha}{\pi} = 1.001743$ . In fact we get  $1.001733 \pm 2.8 \times 10^{-5}$ . The agreement is thus better than  $10^{-4}$ . We can thus conclude that SANC is “commissioned” for the  $Z$  decay.

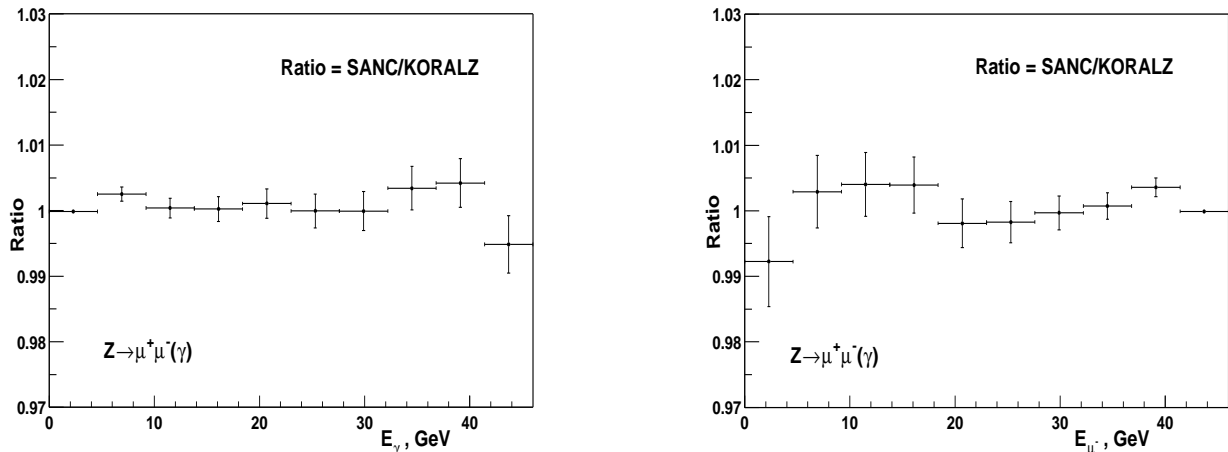


Figure 1: Comparisons (ratios) of the SANC and KORALZ predictions for the  $Z$  decay. Observables **A** and **B**: ratios of the photon energy (left-hand side) and muon energy (right-hand side) distributions from the two programs. The dominant contribution is of leading-log (collinear) nature.

In the case of the  $W$  and Higgs decay we rely on the comparison with PHOTOS. Due to the incomplete one-loop QED in PHOTOS we cannot, in principle, expect the agreement for the decay distributions **A**, **B** to be better than the order of  $\frac{1}{\ln m_B^2/m_\mu^2} \simeq 7\%$ . We see in fig. 3 for Higgs boson decay and in fig. 5 for  $W$  decay, that this is indeed the case. In fact, the agreement is much better in the case of the Higgs boson decay. In figs. 4 and 6 we see the angular distributions of the photon with respect to the charged fermion (observable **C**). Here, in principle, the agreement should not be worse than  $\frac{1}{\ln m_B/E_\gamma^{min}} \simeq 20\%$  for the photon emitted in directions far from the charged particle and  $\frac{1}{\ln m_B^2/m_\mu^2 \ln m_B/E_\gamma^{min}} \simeq 1.4\%$  for directions close to the charged particle. This is indeed the case.

#### 4. Physical uncertainties of PHOTOS in $W$ and $H$ decay

In the case of testing  $H$  and  $W$  decays, the comparisons of PHOTOS with the “matrix-element” type calculations were never accounted for in a well documented way. The following discussion will give us a chance systematically evaluate uncertainties of PHOTOS for these two decays.

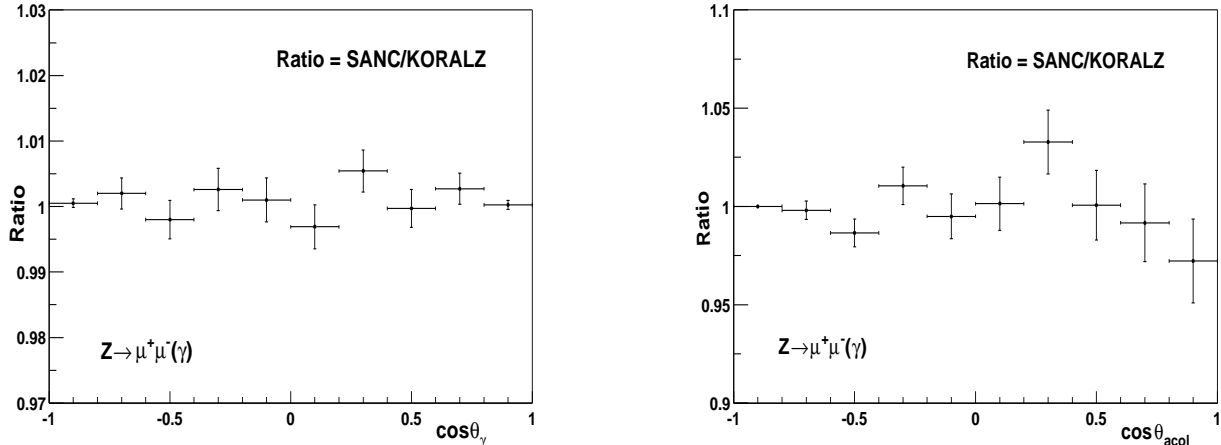


Figure 2: Comparisons (ratios) of the SANC and KORALZ predictions for the  $Z$  decay. Observables **C** and **D**: ratios of the photon angle with respect to  $\mu^-$  (left-hand side) and  $\mu^-\mu^+$  acollinearity (right-hand side) distributions from the two programs. The dominant contribution is of infrared non-leading-log nature for the left-hand side plot, and non-infrared non-leading-log nature for the right-hand side one.

In the case of the Linear Collider studies and many scenarios for new physics, the cross section for the production of the Higgs boson can be quite large. In the case of sophisticated observables, the reconstruction of the reference frames of the intermediate states requires good control of the bremsstrahlung corrections. Our comparison shows that, in the case of the Higgs boson decay, the approximation used in PHOTOS works much better than could be expected from its design principles. In fact it provides results difficult to distinguish from the “matrix-element” ones in the case of all observables **A** to **D** (figs. 3 and 4).

At LEP2, the production and decay of  $W$  pairs is now being combined for all four LEP2 experiments, and uncertainties due to bremsstrahlung in  $W$  decay are important. PHOTOS is part of one of the main programs (YFSWW3) used in the LEP2 analysis of the  $W$ -pair data. Our tests will provide an estimate of the size of the uncertainties, due to use of PHOTOS. If they turn out to be sizeable, the improvements will need to be implemented either into the PHOTOS algorithm or by other means.

In figs. 5 and 6, we see that up to leading order, the distributions agree with the “matrix element” results provided by SANC. There is, however, no exceptionally good agreement observed in the previous case of  $H$  decay.

This point requires further study, before planning improvements of PHOTOS. In particular, a comparison of PHOTOS with another available matrix-element calculation of  $\tau \rightarrow e\nu\bar{\nu}(\gamma)$ , e.g. from TAUOLA [18], should also be repeated to check if a pattern of

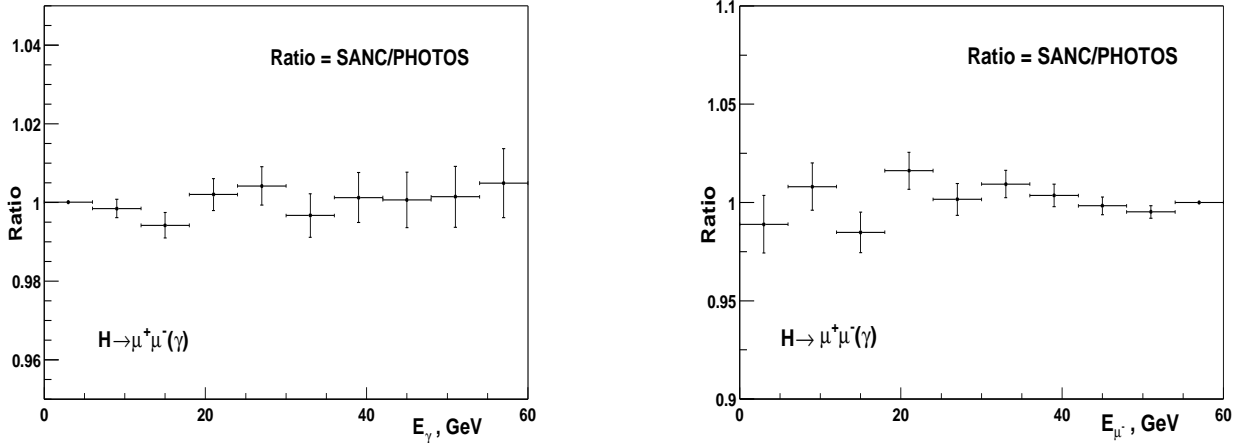


Figure 3: Comparisons (ratios) of the SANC and PHOTOS predictions for the  $H$  decay. Observables **A** and **B**: ratios of the photon energy (left-hand side) and muon energy (right-hand side) distributions from the two programs. The dominant contribution is of leading-log (collinear) nature.

discrepancy similar to that for  $W$  decay is observed. The  $W$  channel is of importance for some studies [19] of LHC Higgs discovery potential as well, see also [20].

## 5. Summary

We have successfully tested SANC versus KORALZ in case of the  $Z$  decay. In this way we have verified the technical correctness of SANC, e.g. its phase-space generation and QED correction amplitudes.

In case of  $W$  and  $H$  decays, we have checked that SANC agrees with the leading order QED calculation provided by the PHOTOS Monte Carlo. These comparisons allow us to evaluate the size of missing non-leading terms in PHOTOS. In the case of  $H$  decays, we have found that PHOTOS results are exceptionally good – differences with SANC are indistinguishable from zero and below 1% everywhere. In the case of  $W$  decay, PHOTOS predictions are within 7% for the end parts of the spectra affected by the leading-log corrections and within 20% for the angular part of the distributions, where the infrared-induced logarithm dominates over non-infrared non-leading terms only. The differences are up to 40% in the phase-space regions where only non-leading corrections contribute to the matrix element. We can conclude that results from all three programs for all four observables agree within the expected precision ranges.

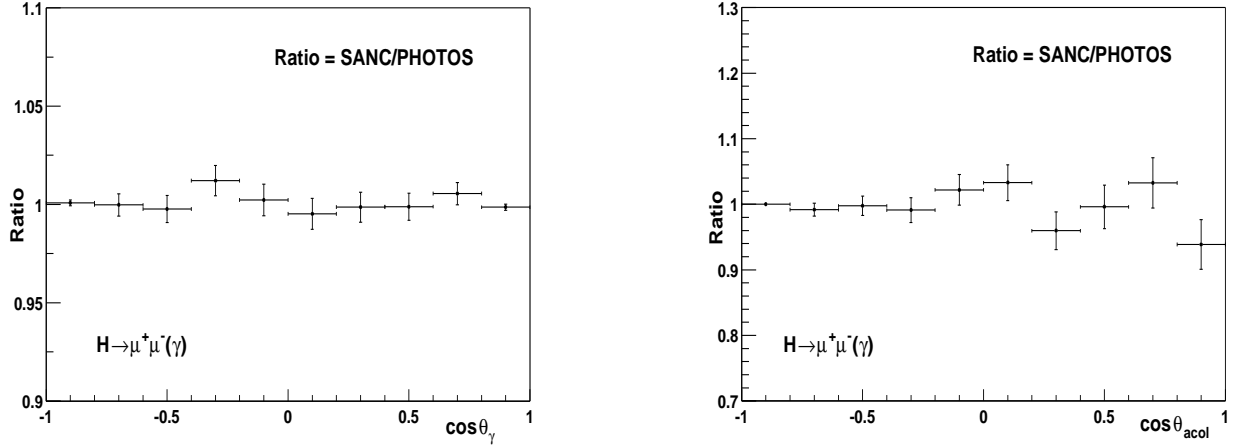


Figure 4: Comparisons (ratios) of the SANC and PHOTOS predictions for the  $H$  decay. Observables **C** and **D**: ratios of the photon angle with respect to  $\mu^-$  (left-hand side) and  $\mu^- \mu^+$  acollinearity (right-hand side) distributions from the two programs. The dominant contribution is of infrared non-leading-log nature for the left-hand side plot, and non-infrared non-leading-log nature for the right-hand side one.

## Acknowledgements

The authors would like to thank D. Bardin and B.F.L. Ward for useful discussions.

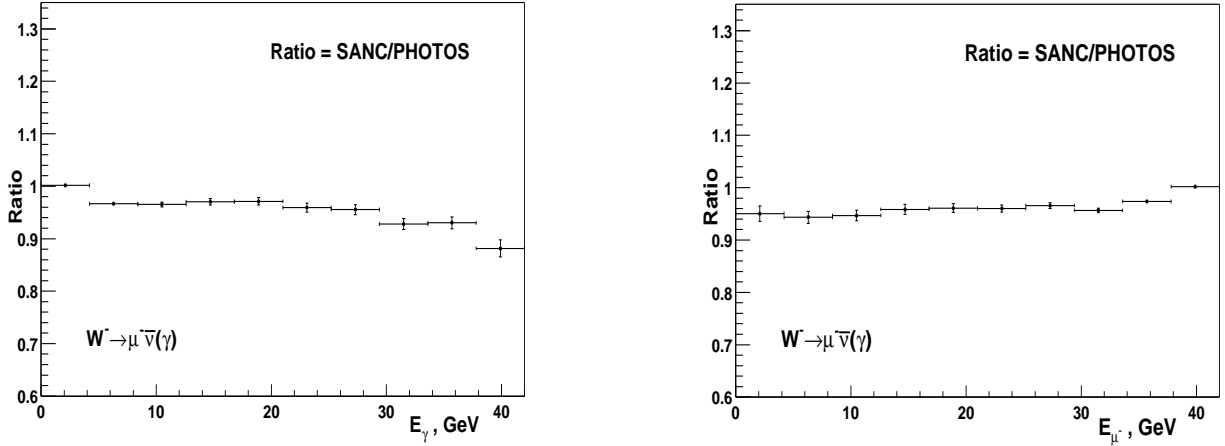


Figure 5: Comparisons (ratios) of the SANC and PHOTOS predictions for the  $W$  decay. Observables **A** and **B**: ratios of the photon energy (left-hand side) and muon energy (right-hand side) distributions from the two programs. The dominant contribution is of leading-log (collinear) nature.

## References

- [1] D. Bardin *et al.*, “Project SANC (former CalcPHEP): Support of analytic and numeric calculations for experiments at colliders”, CERN-TH/2002-245, hep-ph/0209297, to be published in ICHEP2002 Proceedings; D. Bardin *et al.*, “Project CalcPHEP: Calculus for precision high energy physics”, hep-ph/0202004, CAAP-2001 Proceedings, Dubna 2001.
- [2] M. Kobel *et al.*, “Two Fermion Working Group Collaboration”, hep-ph/0007180.
- [3] D. Y. Bardin and G. Passarino, *The standard model in the making: Precision study of the electroweak interactions* (Clarendon Oxford, UK, 1999), 685 p.
- [4] J. A. M. Vermaseren, “New features of FORM”, math-ph/0010025.
- [5] D. Bardin *et al.*, *Comput. Phys. Commun.* **133** (2001) 229, hep-ph/9908433.
- [6] G. Montagna, O. Nicrosini, F. Piccinini and G. Passarino, *Comput. Phys. Commun.* **117** (1999) 278, hep-ph/9804211.
- [7] J. Kublbeck, M. Bohm and A. Denner, *Comput. Phys. Commun.* **60** (1990) 165; T. Hahn and M. Perez-Victoria, *Comput. Phys. Commun.* **118** (1999) 153, hep-ph/9807565;



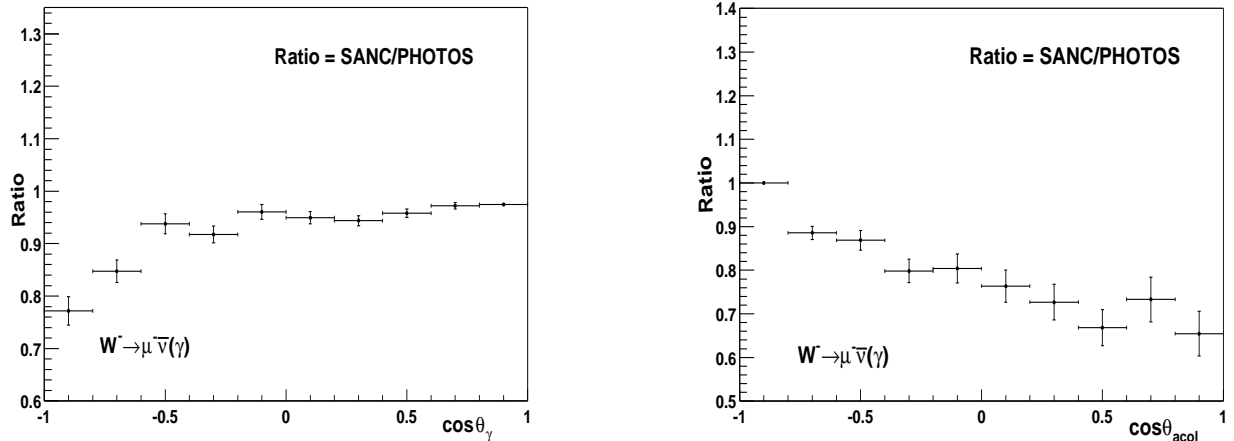


Figure 6: Comparisons (ratios) of the SANC and PHOTOS predictions for the  $W$  decay. Observables **C** and **D**: ratios of the photon angle with respect to  $\mu^-$  (left-hand side) and  $\mu^- \mu^+$  acollinearity (right-hand side) distributions from the two programs. The dominant contribution is of infrared non-leading-log nature for the left-hand side plot, and non-infrared non-leading-log nature for the right-hand side one.

T. Hahn, *Nucl. Phys. Proc. Suppl.* **89** (2000) 231, hep-ph/0005029 and *Comput. Phys. Commun.* **140** (2001) 418-431, hep-ph/0012260;  
T. Hahn and C. Schappacher, *Comput. Phys. Commun.* **143** (2002) 54, hep-ph/0105349.

- [8] D. Bardin, L. Kalinovskaya and G. Nanava, “An electroweak library for the calculation of EWRC to  $e^+e^- \rightarrow f\bar{f}$  within the CalcPHEP project”, CERN-TH/2001-308, hep-ph/0012080.
- [9] A. Andonov, D. Bardin, S. Bondarenko, P. Christova, L. Kalinovskaya and G. Nanava, “Further study of the  $e^+e^- \rightarrow f\bar{f}$  process with the aid of the CalcPHEP system”, CERN-TH/2002-068, hep-ph/0202112.
- [10] A. Andonov, D. Bardin, S. Bondarenko, P. Christova, L. Kalinovskaya and G. Nanava, hep-ph/0207156, to appear in *Particles and Nuclei*.
- [11] S. Jadach, B.F.L. Ward and Z. Was, *Comput. Phys. Commun.* **79** (1994) 503.
- [12] E. Barberio and Z. Was, *Comput. Phys. Commun.* **79** (1994) 291.
- [13] E. Barberio, B. van Eijk and Z. Was, *Comput. Phys. Commun.* **66** (1991) 115.
- [14] F.A. Berends, R. Kleiss and S. Jadach, *Comput. Phys. Commun.* **29** (1983) 185.

- [15] S. Jadach and Z. Was, *Comput. Phys. Commun.* **64** (1991) 267.
- [16] S. Jadach and Z. Was, *Comput. Phys. Commun.* **36** (1985) 191.
- [17] S. Jadach and Z. Was, *Acta Phys. Polon.* **B15** (1984) 1151.
- [18] M. Jeżabek, Z. Was, S. Jadach and J.H. Kühn, *Comput. Phys. Commun.* **70** (1992) 69.
- [19] E. Richter-Was, *Z. Phys. C* **61** (1994) 323.
- [20] ATLAS collaboration, “ ATLAS Detector and Physics Performance Technical Design Report”, CERN/LHCC/99-15, vol. 2, p. 674–735.